# Micromechanics of Hydrogen-Assisted Damage in Progressively Drawn Pearlitic Steel

**J. Toribio[1], F. J. Ayaso[2] and E. Ovejero[3]**

[1] Department of Materials Engineering, University of Salamanca, Spain
[2] Department of Materials Science, University of La Coruña, Spain
[3] Intitute of Materials Technology of Asturias, Spain

**ABSTRACT:** *This paper analyzes the evolution of hydrogen-assisted damage topography in progressively drawn pearlitic steels. The fractographic analysis revealed changes in the microscopic topographies depending on the fracture propagation mode, with an evolution from pure tearing topography surface (TTS) in slightly drawn steels to a kind of very deformed TTS (in direction of cold drawing or wire axis) in heavily drawn steels. An image analysis technique was used to analyze the different microscopic fracture modes, thus finding correlations between them. Results showed that the very deformed TTS really observed in heavily drawn steels could be virtually obtained by deforming –in the drawing direction– the micrograph of slightly drawn steels. This fact provides bases to elucidate the real physical micromechanism of hydrogen-assisted fracture in pearlitic steels.*

## INTRODUCTION

Cold drawn eutectoid steels are high-strength materials used as constituents of prestressed concrete structures. Previous research [1,2] dealt with the fracture of these materials in aggressive environment, showing that heavily drawn prestressing steels exhibit anisotropic fracture behavior associated with changes in the crack propagation direction and transition from mode I to mixed mode propagation approaching the wire axis direction.

In more recent works [3,4] this research line has been developed to analyze steels with intermediate degree of cold drawing, in order to relate – in the materials science manner– the macroscopic behavior of the steels with their microstructure at the two basic microstructural levels of the pearlite colonies [5,6] and the pearlitic lamellar microstructure [7,8], as a function of the cold drawing degree achieved during the manufacturing process to produce the final commercial product.

This paper goes further in the research line and studies –by means of image analysis techniques– the evolution of hydrogen-assisted microdamage topographies at the microscopic levels for the different degrees of cold

drawing, in order to elucidate the physical micromechanisms of fracture of pearlitic steels in hydrogen environments, considering the progressively anisotropic fracture behaviour as the cold drawing level increases.


## MATERIALS AND MICROSTRUCTURE

The materials used in this work were high-strength steels taken from a real manufacturing process. Wires with different degrees of cold drawing were obtained by stopping the manufacturing chain and taking samples from the intermediate stages. Table 1 shows the chemical composition common to all steels, and Table 2 includes the diameter ($D_i$), the yield strength ($\sigma_Y$), the ultimate tensile stress ($\sigma_R$) and the fracture toughness ($K_{IC}$). The name of each steel indicates the number of cold drawing steps which has undergone.

TABLE 1: Chemical composition (wt%) of the steels

| C | Mn | Si | P | S | Cr | V | Al |
|------|------|------|-------|-------|-------|-------|-------|
| 0.80 | 0.69 | 0.23 | 0.012 | 0.009 | 0.265 | 0.060 | 0.004 |

TABLE 2: Diameter reduction and mechanical properties of the steels

| Steel | 0 | | 1 | | 2 | | 3 |
|-------|-------|-------|-------|-------|-------|-------|-------|
| $D_i$ (mm) | 12.00 | 10.80 | 9.75 | 8.90 | 8.15 | 7.50 | 7.00 |
| $\sigma_Y$ (GPa) | 0.686 | 1.100 | 1.157 | 1.212 | 1.239 | 1.271 | 1.506 |
| $\sigma_R$ (GPa) | 1.175 | 1.294 | 1.347 | 1.509 | 1.521 | 1.526 | 1.762 |
| $K_{IC}$ (MPam$^{1/2}$) | 60.1 | 61.2 | 70.0 | 74.4 | 110.1 | 106.5 | 107.9 |

The microstructural evolution with cold drawing was studied in previous woks [5-8], analyzing the evolution with cold drawing of the two basic microstructural levels: the pearlite colonies (first level) and the pearlitic lamellae (second level). With regard to the first, a progressive elongation and orientation of the pearlitic colonies in the cold drawing direction (wire axis) was observed [5,6]. In the matter of the second, the analysis showed an increasing closeness of packing (with decrease of the interlamellar spacing) and a progressive orientation of the pearlitic lamellar microstructure in the cold drawing direction [7,8]. Therefore, both pearlite colonies and pearlitic lamellar microstructure tend to align to a direction quasi-parallel to the wire axis as cold drawing proceeds. Figure 1 (cf.[8]) shows the pearlitic microstructure of steels 0 and 6 respectively, by means of micrographs

corresponding to longitudinal metallographic sections of the wires (those sections containing the wire axis). It is seen that, while the microstructure of steel 0 (hot rolled bar which is not cold drawn at all) is randomly oriented, the microstructure of steel 6 (prestressing steel heavily cold drawn) is markedly oriented in the direction of the wire axis (or cold drawing direction) which corresponds to the vertical side of the micrographs. Figure 2 plots the quantification of this orientation effect at the levels of colonies and lamellae respectively.



| (a) | (b) |
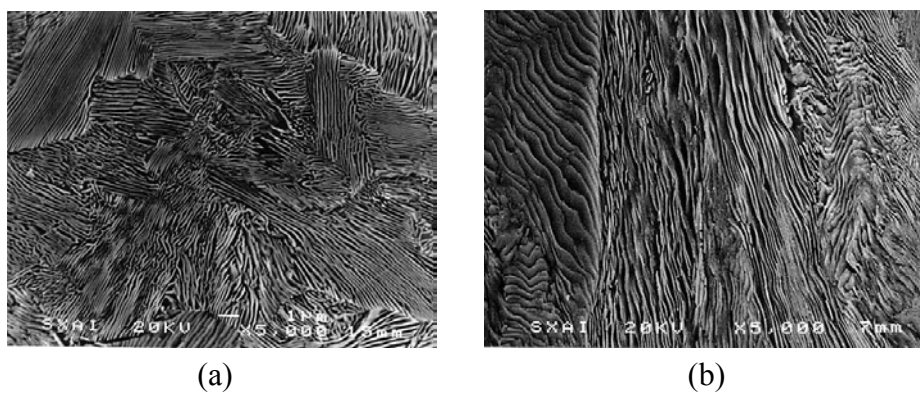
**Figure 1:** Longitudinal metallographic sections showing the microstructure of steel 0 (a) and steel 6 (b), where the cold drawing direction is vertical.



| (a) | (b) |
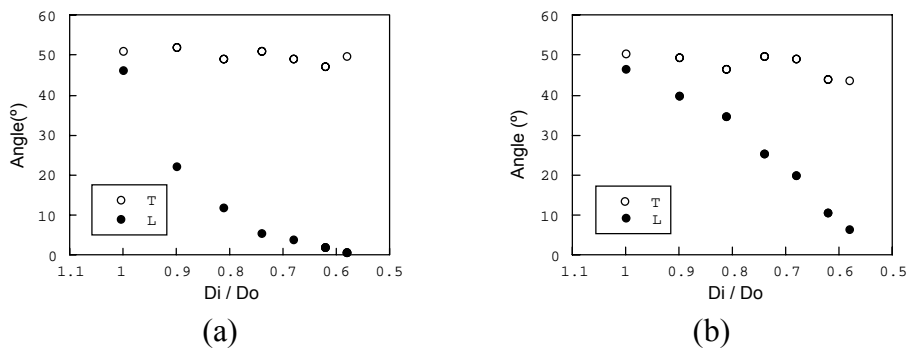
**Figure 2:** Evolution with cold drawing of the orientation angles of pearlite colonies (a) and lamellae (b), in the longitudinal (L) and transverse (T) metallographic sections. In (a) the angle was measured between the major axis of the colony (modeled as an ellipsoid) and the axial direction (L section) or the radial one (T section). In (b) the angle was measured between the direction of the lamellae in the metallographic cut and the axial direction.

## EXPERIMENTAL PROGRAM

To analyze the hydrogen assisted cracking (HAC) behavior of the different steels, slow strain rate tests were performed on precracked steel wires. After precracking with $K_{max} = 0.30K_{IC}$, samples were placed in a corrosion cell containing aqueous solution of 1g/l $Ca(OH)_2$ plus 0.1g/l NaCl (pH=12.5). Tests were conducted under potentiostatic control at $-1200$ mV vs. SCE at which the environmental mechanism is HAC [1]. The applied displacement rate was constant during each test and proportional to each wire diameter: 1.7 x$10^{-3}$ mm/min for steel 6 and 3.0 x$10^{-3}$ mm/min for steel 0.

The experimental results showed an important fact: the HAC behaviour becomes more anisotropic as the cold drawing degree increases, as depicted in Figure 3 by means of the *fracture profile* (macroscopic topography of the fracture surface). Thus a transverse crack tends to change its propagation direction to approach the wire axis or cold drawing direction and an initial mode I growth evolves towards a mixed mode propagation (*strength anisotropy* with regard to HAC).
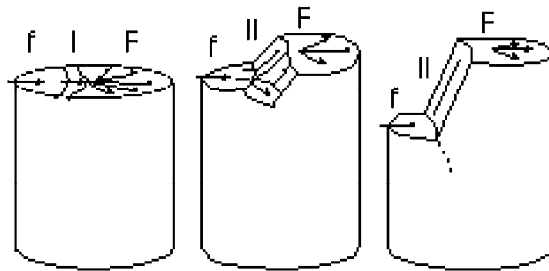


**Figure 3:** Evolution with cold drawing of fracture surfaces in HAC, from slightly to heavily drawn steels (left to right). Increasingly anisotropic behaviour with cold drawing (f: fatigue; I: mode I propagation; II: mixed mode propagation; F: final fracture by cleavage).

## FRACTOGRAPHIC ANALYSIS

A fractographic analysis by scanning electron microscopy (SEM) was carried out on the fracture surfaces to elucidate the microscopic modes of fracture. Figure 4 offers the microscopic topographies for hot rolled bar (steel 0 which is not cold drawn at all) and for a heavily drawn prestressing steel (steel 6 which has suffered six steps of cold drawing).

(a)                                              (b)
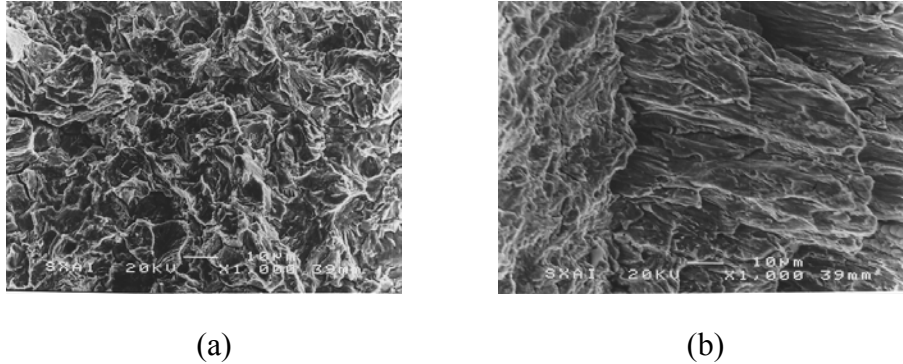
**Figure 4:** Microscopic fracture modes in steel 0 (a) and steel 6 (b).

In the hot rolled bar (steel 0) there is a subcritical crack growth in mode I by *tearing topography surface* (TTS, cf. [9-12]) before the unstable cleavage-like propagation associated with mechanical final fracture. This special microscopic fracture mode is undoubtedly associated with hydrogen-assisted micro-damage in steels with pearlitic microstructure [11-12].

In the heavily drawn prestressing steel wire (steel 6) the microscopic fracture mode is a kind of *very deformed* TTS, the deformation axis coincident with the cold drawing direction. This topography is produced as a consequence of the macroscopic crack deflection with mode II propagation, *as if* a previous TTS mode had been strained by shear in its own fracture plane (quasi-parallel to the drawing axis).

The microscopic fracture modes of Figure 4 may be classified as *hydrogen damage topographies* (HDT). The appearance of this generic topography is a function of the degree of drawing so that it can be noted as $HDT^{(i)}$, where $i$ is the number of cold drawing steps undergone by the steel. Thus the topography $HDT^{(i)}$ evolves form pure TTS (which corresponds *exactly* with the mode described in [9-12]) in steel 0 to $HDT^{(6)}$ (a kind of TTS *very deformed* in the wire axis or cold drawing direction) in steel 6. Between them, a wide range of HDT topographies with intermediate degree of deformation was observed.

**DISCUSSION**

Form the observation of the fractographs corresponding to $HDT^{(0)}$ (Figure 4a) and $HDT^{(6)}$ (Figure 4b), the following statements may be drawn:

- All the HDT modes for different degrees of cold drawing are associated to the same HAC mechanism (cathodic potentials and decrease of stress intensity factor).

- A generic HDT$^{(i)}$ exhibits an *apparent deformation* (in the fractograph) which is an increasing function of the degree of cold drawing (represented by the superindex *i* which indicates the number of cold drawing steps undergone by the steel).

- Such a deformation seems to be oriented in the direction of the larger size of the fractograph, i.e., in a direction quasi-parallel to the wire axis or cold drawing direction.

Thus the question arises about whether or not a geometric relationship does exist between the HDT modes so that one can be *virtually* obtained by deformed a previous one (associated with a lower degree of cold drawing). This virtual transformation is sketched in Figure 5a, in which the initial fractograph HDT$^{(0)}$ (or pure TTS) in the hot rolled bar is virtually oriented in the direction of HAC in the cold drawn material and deformed by transformations in the radial, hoop and axial directions.

The parameters of the geometric transformations are obtained by the hypothesis of conservation of volume in the Plasticity theory and represent *the virtual deformation* which should be applied to the HDT$^{(i)}$ to obtain other HDT$^{(j)}$ (j > i). Figure 5b shows the results of this virtual deformation process to obtain HDT$^{(6)}$ from HDT$^{(4)}$, where it is seen that this virtual topography really resembles the real one shown in Figure 4b, which confirms that the micromechanism of fracture is similar in both cases.


## CONCLUSIONS


In eutectoid steels, the microstructural changes produced by the cold drawing process affect the macroscopic behavior with regard to environmentally assisted cracking in general and hydrogen assisted cracking (or hydrogen embrittlement) in particular.

In heavily drawn steels, the microscopic fracture mode is a kind of very deformed tearing topography surface, the deformation axis coincident with the cold drawing direction. This topography is produced as a consequence of the macroscopic crack deflection with mode II propagation.

A proportional relationship was found between the different hydrogen damage topographies (HDT): the very deformed TTS *really* observed in heavily drawn steels could be *virtually* obtained by deforming the

micrograph of the pure TTS (associated with the hot rolled material) in the direction of cold drawing.



(a)                                        (b)
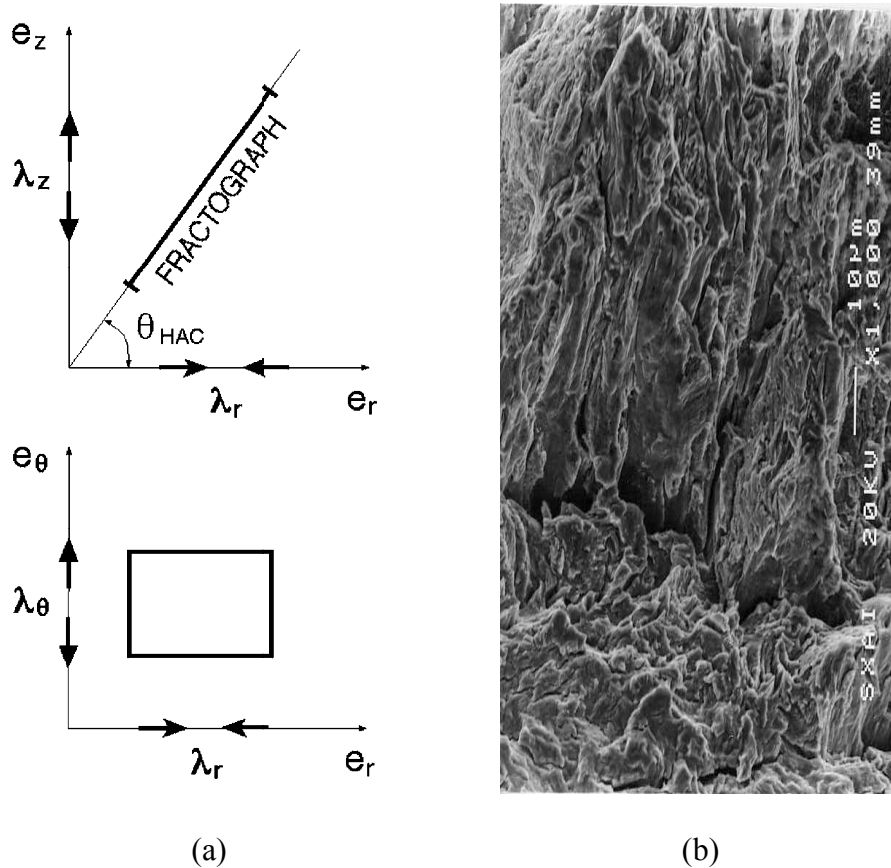
**Figure 5:** (a) *Virtual* deformation of the fractograph; (b)*Virtual* HDT[6] obtained by computer deformation of HDT[4] in the cold drawing direction.

**REFERENCES**

1. Parkins, R.N., Elices, M., Sánchez-Gálvez, V. y Caballero, L. (1982) *Corrosion Science* **22**, 379.
2. Lancha, A.M. (1987) Ph. D. Thesis, Complutense University of Madrid.
3. Toribio, J. and Ovejero, E. (1998) *International Journal of Fracture* **90**, L21.
4. Toribio, J. and Ovejero, E. (1999) *Scripta Materialia* **40**, 943.
5. Toribio, J. and Ovejero, E. (1997) *Materials Science and Engineering* **A234-236**, 579.
6. Toribio, J. and Ovejero, E. (1998) *Journal of Materials Science Letters* **17**, 1037.
7. Toribio, J. and Ovejero, E. (1998) *Scripta Materialia* **39**, 323.
8. Toribio, J. and Ovejero, E. (1998) *Mechanics of Time-Dependent Materials* **1**, 307.
9. Thompson, A. W. and Chesnutt, J.C. (1979) *Metallurgical Transactions* **10A**, 1193.
10. Costa, J.E. and Thompson, A.W. (1982) *Metallurgical Transaction*s **13A**, 1315.
11. Toribio, J., Lancha, A.M. and Elices, M. (1991) *Scripta Metalurgica et Materialia* **25**, 2239.
12. Toribio, J., Lancha, A.M. and Elices, M. (1992) *Metallurgical Transactions* **23A**, 157.